

## Impact of Transverse Mode Resonances on Second Harmonic (H2) Generation in RF BAW Structures

RF BAW 構造中の 2 次高調波発生に対する横モードの影響

Luyan Qiu<sup>1†</sup>, Xinyi Li<sup>2,1</sup>, Tatsuya Omori<sup>1</sup>, and Ken-ya Hashimoto<sup>1</sup>

(<sup>1</sup>Chiba University, <sup>2</sup>University of Electronic Science and Technology of China)

邱魯岩<sup>1†</sup>, 李昕熠<sup>2,1</sup>, 大森達也<sup>1</sup>, 橋本研也<sup>1</sup> (<sup>1</sup>千葉大学, <sup>2</sup>電子科技大学)

### 1. Introduction

Currently, nonlinearity reduction is one of the biggest concerns for performance enhancement of radio frequency (RF) surface and bulk acoustic wave (SAW/BAW) duplexers and/or multiplexers to guarantee the receiver sensitivity under incidence of strong signals.[1-3] Yang, et al., reported that spurious resonances such as transverse modes sometimes cause very strong second-order nonlinearity in RF BAW devices.[4]

Hashimoto and Li proposed use of the  $h$ -form piezoelectric constitutive equations for the one-dimensional (1D) perturbation analysis of nonlinear signal generation in RF BAW devices, and showed that second-order nonlinearity of the main mode can be simulated well[5] without use of time-consuming harmonic balance technique[6].

In the paper, this analysis is extended to the two-dimensional (2D) case, and influence of transverse mode resonances is discussed to second harmonic (H2) generation.

### 2. Analysis procedures

Fig. 1 shows a 2D model of a free-standing BAW resonator comprising an AlN piezoelectric layer sandwiched in between two Ru electrodes[7]. The lateral dimension of the resonator is much larger than thickness. The side edges of resonator are assumed to be clamped to make the analysis simple and generate strong transverse resonances.

Resistivity of electrodes is ignored, and thus the electrodes can be excluded from the simulation in the Maxwell equation. Besides, the acoustic loss is also added to piezo-layer and metal electrodes respectively so as to adjust the Q factor.

First, linear analysis is performed for a given driving frequency  $\omega$  by conventional 2D finite element method (FEM). For the calculation, the COMSOL Multiphysics is used. From the obtained input admittance, voltage across the resonator is estimated by taking external circuit conditions into account, and wave fields strain  $S$  and electric flux density  $D$  in the resonator body are determined.

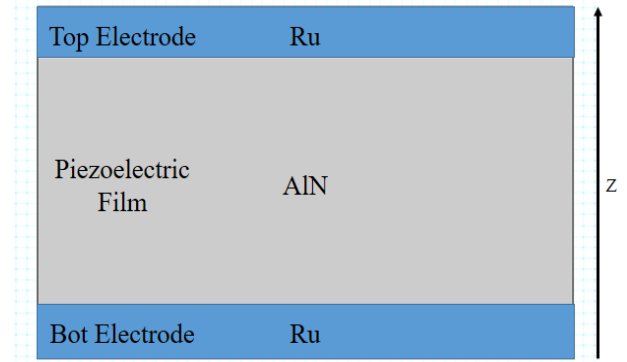


Fig.1 Cross sectional view of an RF BAW resonator

Second, stress  $T$  and electric field  $E$  generated by nonlinearity are estimated. Following to [5], the following  $h$ -form piezoelectric constitutive equations are used:

$$T = c^D S - hD + T_N(S, D) \quad (1)$$

and

$$E = \beta^S D - hS + E_N(S, D). \quad (2)$$

where  $c^D$ ,  $h$  and  $\beta^S$  are stiffness at constant  $D$ , piezoelectric constant, and inverse permittivity at constant  $S$ , respectively.

Expansion of  $T_N$  and  $E_N$  to the second order gives:

$$T_N = -\frac{1}{2} \chi_{20}^T S^2 - \chi_{11}^T DS - \frac{1}{2} \chi_{02}^T D^2 \quad (3)$$

and

$$E_N = -\frac{1}{2} \chi_{11}^T S^2 - \chi_{02}^T DS - \frac{1}{2} \chi_{02}^E D^2. \quad (4)$$

In the perturbation analysis,  $T_N$  and  $E_N$  are evaluated by substituting  $S$  and  $D$  estimated by the linear analysis for  $\omega$  into Eqs. (3) and (4).

Since  $T_N$  and  $E_N$  has already be determined, Eq. (1) and (2) can be converted into the  $e$ -form as:

$$T = c^E S - eE + (eE_N + T_N) \quad (5)$$

and

$$D = \varepsilon^S E - eS - \varepsilon^S E_N \quad (6)$$

<sup>†</sup>keew@chiba-u.jp

where  $c^E$ ,  $e$  and  $\varepsilon^S$  are stiffness at constant  $E$ , piezoelectric constant, and permittivity at constant  $S$ , respectively. Then substitution into Newton's law and Gauss's law give

$$\nabla \cdot (c^E S - eE) - \rho \ddot{u} = -\nabla \cdot (eE_N + T_N) \quad (7)$$

and

$$\nabla \cdot (\varepsilon^S E - eS) = \nabla \cdot (\varepsilon^S E_N). \quad (8)$$

Eqs. (7) and (8) are linear partial differential equations when the right-side terms are regarded as body sources with the frequency  $2\omega$ . Then linear 2D FEM analysis is again applicable.

The voltage difference between two electrodes is set at zero, and the FEM analysis is performed. Then total charge induced to the top electrode is evaluated. Since admittance of the resonator can be also calculated for  $2\omega$ , we can evaluate H2 voltage by taking external circuit conditions into account.

### 3. Numerical example

Parameters appearing Eqs. (3) and (4) are unknown. Furthermore,  $S$  and  $D$  are tensors. Here only  $S_{33} = \partial u_3 / \partial z$  and  $D_3$  are taken into account in these equations because they are expected to be dominant for both the main and transverse mode resonances under concern. In this work,  $\chi_{11}^T$  and  $\chi_{20}^T$  was considered.

Fig. 2 shows impedance of the RF BAW resonator obtained by the linear analysis. In order to fit with real device characteristics, the parasitic capacitance was added in parallel. Transverse resonance can be seen at frequencies lower than the resonance. The figure also shows the impedance at the harmonic frequency. No acoustic resonance is seen in this frequency range.

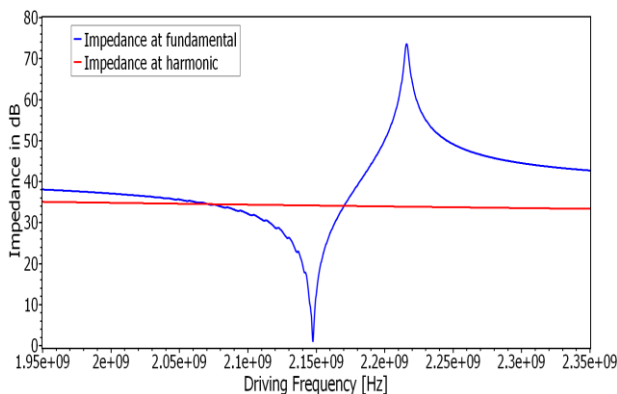


Fig.2 Impedance of the RF BAW resonator

Fig. 3 shows simulated H2 response for the RF BAW resonator. For comparison, that obtained by

the 1D simulation is also shown. It is seen these 1D and 2D calculations are almost identical near the H2 peak. However, H2 responses become considerably strong at the frequency region where transverse resonances occur. The result obtained by  $\chi_{11}^T$  is similar to that obtained by  $\chi_{20}^T$ . Anyway, this phenomenon is what we have seen experimentally[1,2,4].

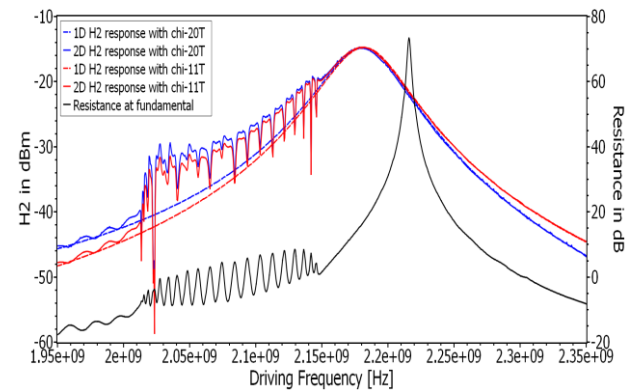


Fig.3 Simulated 2D H2 output vs. 1D H2 output and resistance at fundamental frequencies

### 4. Conclusion

This paper proposed 2D perturbation analysis of nonlinear signal generation in RF BAW devices, and impact of transverse modes to H2 generation was discussed. In this analysis, nonlinear parameters  $\chi_{20}^T$  and  $\chi_{11}^T$  were considered. The result shows that this method can predict H2 emissions.

### Acknowledgement

The author thanks Dr. M.Ueda and Mr. T.Nishihara of Taiyo Yuden, Co. Ltd. for their fruitful discussions.

### References

1. D.Feld, et al., Proc. IEEE Ultrason Symp (2009) pp. 1082-1087
2. D.S.Shim, et al., International Journal of RF and Microwave Computer-Aided Engineering, **21** (2011) p. 486
3. R.Nakagawa, et al., Jpn. J. Appl. Phys., **55** (2016) 07KD02
4. T.Yang, et al., Proc. IEEE Ultrason Symp (2017) 10.1109/ULTSYM.2017.8092136
5. K.Hashimoto, et al., Proc. IEEE Freq. Contr. Symp. (2017) 10.1109/FCS.2017.8088951
6. H.G.Brachtendorf, et al., Proc. International Symp. on Circuits and Systems (1995) p. 1388.
7. S.Taniguchi, et al., Proc. IEEE Ultrason. Symp. (2007) pp. 600-603